Physics Letters B 746 (2015) 237–241

Contents lists available at ScienceDirect

Physics Letters B

www.elsevier.com/locate/physletb

Relating the small parameters of neutrino oscillations

Soumita Pramanick, Amitava Raychaudhuri

Department of Physics, University of Calcutta, 92 Acharya Prafulla Chandra Road, Kolkata 700009, India

ARTICLE INFO

Article history:
Received 1 March 2015
Received in revised form 3 May 2015
Accepted 3 May 2015
Available online 6 May 2015
Editor: J. Hisano

Keywords:
Neutrino mixing
θ_{13}
Leptonic CP-violation
Neutrino mass ordering
Perturbation

ABSTRACT

Neutrino oscillations reveal several small parameters, namely, θ_{13}, the solar mass splitting *vis-à-vis* the atmospheric one, and the deviation of θ_{23} from maximal mixing. Can these small quantities all be traced to a single source and, if so, how could that be tested? Here a see-saw model for neutrino masses is presented wherein a dominant term generates the atmospheric mass splitting with maximal mixing in this sector, keeping $\theta_{13} = 0$ and zero solar splitting. A Type-I see-saw perturbative contribution results in non-zero values of θ_{13}, Δm^2_{solar}, θ_{12}, as well as allows θ_{23} to deviate from $\pi/4$ in consistency with the data while interrelating them all. CP-violation is a natural consequence and is large ($\delta \sim \pi/2, 3\pi/2$) for inverted mass ordering. The model will be tested as precision on the neutrino parameters is sharpened.

Information on neutrino mass and mixing have been steadily emerging from oscillation experiments. Among them the angle[1] θ_{13} is small ($\sin\theta_{13} \sim 0.1$) [1] while global fits to the solar, atmospheric, accelerator, and reactor neutrino oscillation data indicate that θ_{23} is near maximal ($\sim \pi/4$) [2,3]. On the other hand, the solar mass square difference is two orders smaller than the atmospheric one. These mixing parameters and the mass ordering are essential inputs for identifying viable models for neutrino masses.

A natural choice could be to take the mixing angles to be initially either $\pi/4$ (θ_{23}) or zero (θ_{13}, θ_{12}) and the solar splitting absent. In this spirit, here a proposal is put forward under which the atmospheric mass splitting and maximal mixing in this sector arise from a zero-order mass matrix while the smaller solar mass splitting and realistic θ_{13} and θ_{23} are generated by a Type-I see-saw [4] which acts as a perturbation. θ_{12} also arises out of the same perturbation and as a consequence of degeneracy is not constrained to be small. Attempts to generate *some* of the neutrino parameters by perturbation theory are not new [5,6], but to our knowledge there is no work in the literature that indicates that *all* the small parameters could have the same perturbative origin and agree with the current data.

The unperturbed neutrino mass matrix in the mass basis is $M^0 = \mathrm{diag}\{m_1^{(0)}, m_1^{(0)}, m_3^{(0)}\}$ with the mixing matrix of the form

$$U^0 = \begin{pmatrix} 1 & 0 & 0 \\ 0 & \sqrt{\frac{1}{2}} & \sqrt{\frac{1}{2}} \\ 0 & -\sqrt{\frac{1}{2}} & \sqrt{\frac{1}{2}} \end{pmatrix} . \tag{1}$$

Here $\Delta m^2_{atm} = (m_3^{(0)})^2 - (m_1^{(0)})^2$. By suitably choosing the Majorana phases the masses $m_1^{(0)}$, $m_3^{(0)}$ are taken to be real and positive. The columns of U^0 are the unperturbed flavour eigenstates.[2] As stated, $\Delta m^2_{solar} = 0$ and $\theta_{13} = 0$. Since the first two states are degenerate in mass, one can also take $\theta_{12} = 0$. It is possible to generate this mass matrix from a Type-II see-saw.

In the flavour basis the mass matrix is $(M^0)^{flavour} = U^0 M^0 U^{0T}$ which in terms of $m^{\pm} = m_3^{(0)} \pm m_1^{(0)}$ is

$$(M^0)^{flavour} = \frac{1}{2}\begin{pmatrix} 2m_1^{(0)} & 0 & 0 \\ 0 & m^+ & m^- \\ 0 & m^- & m^+ \end{pmatrix} . \tag{2}$$

The perturbation is obtained by a Type-I see-saw. To reduce the number of independent parameters, in the flavour basis the Dirac mass term is taken to be proportional to the identity, i.e.,

$$M_D = m_D \, \mathbb{I} . \tag{3}$$

E-mail addresses: soumitaparamanick5@gmail.com (S. Pramanick), palitprof@gmail.com (A. Raychaudhuri).

[1] For the lepton mixing matrix the standard PMNS form is used.

[2] In the flavour basis the charged lepton mass matrix is diagonal.

http://dx.doi.org/10.1016/j.physletb.2015.05.007

In this basis, in the interest of minimality the right-handed neutrino Majorana mass matrix is taken with only two non-zero complex entries.

$$M_R^{flavour} = m_R \begin{pmatrix} 0 & xe^{-i\phi_1} & 0 \\ xe^{-i\phi_1} & 0 & 0 \\ 0 & 0 & ye^{-i\phi_2} \end{pmatrix} , \tag{4}$$

where x, y are dimensionless constants of $\mathcal{O}(1)$. No generality is lost by keeping the Dirac mass real.

As a warm-up consider first the real case, i.e., $\phi_1 = 0$ or π, $\phi_2 = 0$ or π. For notational convenience in the following the phase factors are not displayed; instead x (y) is taken as positive or negative depending on whether ϕ_1 (ϕ_2) is 0 or π. Negative x and y offer interesting variants which are stressed at the appropriate points.

The Type-I see-saw contribution in the mass basis is:

$$M'^{mass} = U^{0T}\left[M_D^T (M_R^{flavour})^{-1} M_D\right] U^0 = \frac{m_D^2}{\sqrt{2}\, xym_R} \begin{pmatrix} 0 & y & y \\ y & \frac{x}{\sqrt{2}} & -\frac{x}{\sqrt{2}} \\ y & -\frac{x}{\sqrt{2}} & \frac{x}{\sqrt{2}} \end{pmatrix} . \tag{5}$$

The effect on the solar sector is governed by the submatrix of M'^{mass} in the subspace of the two degenerate states,

$$M'^{mass}_{2\times 2} = \frac{m_D^2}{\sqrt{2}\, xym_R} \begin{pmatrix} 0 & y \\ y & x/\sqrt{2} \end{pmatrix} . \tag{6}$$

To first order in the perturbation:

$$\tan 2\theta_{12} = 2\sqrt{2}\left(\frac{y}{x}\right) . \tag{7}$$

For $y/x = 1$ one obtains the tribimaximal mixing value of θ_{12} which, though allowed by the data[3] at 3σ, is beyond the 1σ region. Since for the entire range of θ_{12} one has $\tan 2\theta_{12} > 0$, x and y must be chosen of the same sign. Therefore, either $\phi_1 = 0 = \phi_2$ or $\phi_1 = \pi = \phi_2$. From the global fits to the experimental results one finds:

$$0.682 < \frac{y}{x} < 1.075 \text{ at } 3\sigma . \tag{8}$$

Further, from Eq. (6),

$$\Delta m^2_{solar} = \frac{m_D^2}{xym_R}\, m_1^{(0)} \sqrt{x^2 + 8y^2} . \tag{9}$$

To first order in the perturbation the corrected wave function $|\psi_3\rangle$ is:

$$|\psi_3\rangle = \begin{pmatrix} \kappa \\ \frac{1}{\sqrt{2}}(1 - \frac{\kappa}{\sqrt{2}}\frac{x}{y}) \\ \frac{1}{\sqrt{2}}(1 + \frac{\kappa}{\sqrt{2}}\frac{x}{y}) \end{pmatrix} , \tag{10}$$

where

$$\kappa \equiv \frac{m_D^2}{\sqrt{2}\, xm_R m^-} . \tag{11}$$

For positive x the sign of κ is fixed by that of m^-. Since by convention all the mixing angles θ_{ij} are in the first quadrant, from Eq. (10) one must identify:

$$\sin\theta_{13}\cos\delta = \kappa = \frac{m_D^2}{\sqrt{2}\, xm_R m^-} , \tag{12}$$

[3] We use the 3σ ranges $7.03 \le \Delta m^2_{21}/10^{-5}$ eV$^2 \le 8.03$ and $31.30^\circ \le \theta_{12} \le 35.90^\circ$ [2].

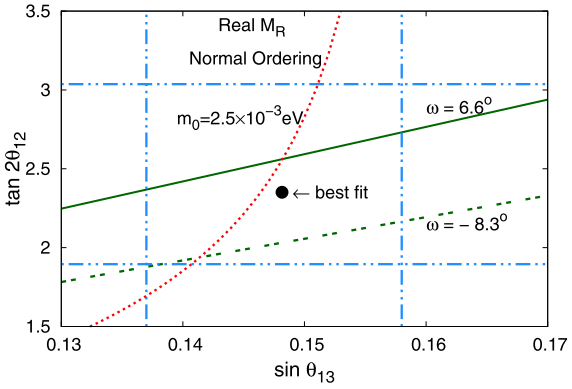

Fig. 1. The blue dot-dashed box is the global-fit 3σ allowed range of $\sin\theta_{13}$ and $\tan 2\theta_{12}$. The best-fit point is shown as a black dot. The red dotted curve is from Eq. (13) with $m_0 = 2.5$ meV when the best-fit values of the two mass-splittings are used. The portion below the green solid (dashed) straight line is excluded by θ_{23} at 3σ – Eq. (17) – for the first (second) octant. In case of inverted ordering no solution of Eq. (13) is allowed for real M_R. (For interpretation of the references to colour in this figure legend, the reader is referred to the web version of this article.)

where for $x > 0$ the PMNS phase $\delta = 0$ for normal mass ordering (NO) and $\delta = \pi$ for inverted mass ordering (IO). Needless to say, both these cases are CP conserving. If x is negative then NO (IO) would correspond to $\delta = \pi$ (0).

An immediate consequence of Eqs. (12), (7), and (9) is

$$\Delta m^2_{solar} = \text{sgn}(x)\, m^- m_1^{(0)}\, \frac{4\sin\theta_{13}\cos\delta}{\sin 2\theta_{12}} , \tag{13}$$

which exhibits how the solar sector and θ_{13} are intertwined. The positive sign of Δm^2_{solar}, preferred by the data, is trivially verified since $\text{sgn}(x)\ m^- \sin\theta_{13}\cos\delta > 0$ from Eq. (12). However, Eq. (13) excludes inverted ordering. Once the neutrino mass square splittings, θ_{12}, and θ_{13} are chosen, Eq. (13) determines the lightest neutrino mass, m_0. Defining $z = m^- m_1^{(0)}/\Delta m^2_{atm}$ and $m_0/\sqrt{|\Delta m^2_{atm}|} = \tan\xi$, one has

$$z = \sin\xi/(1+\sin\xi) \text{ (normal ordering)}, \quad z = 1/(1+\sin\xi) \text{ (inverted ordering)} . \tag{14}$$

It is seen that $0 \le z \le 1/2$ for NO and $1/2 \le z \le 1$ for IO, with $z \to 1/2$ corresponding to quasidegeneracy, i.e., $m_0 \to$ large, in both cases. From Eq. (13)

$$z = \left(\frac{\Delta m^2_{solar}}{|\Delta m^2_{atm}|}\right)\left(\frac{\sin 2\theta_{12}}{4\sin\theta_{13}|\cos\delta|}\right) , \tag{15}$$

with $|\cos\delta| = 1$ for real M_R. As shown below, the allowed ranges of the oscillation parameters imply $z \sim 10^{-2}$ and so inverted mass ordering is disallowed.

From Eq. (10) one further finds:

$$\tan\theta_{23} \equiv \tan(\pi/4 - \omega) = \frac{1 - \frac{\kappa}{\sqrt{2}}\frac{x}{y}}{1 + \frac{\kappa}{\sqrt{2}}\frac{x}{y}} , \tag{16}$$

where, using Eqs. (7) and (12),

$$\tan\omega = \frac{2\sin\theta_{13}\cos\delta}{\tan 2\theta_{12}} . \tag{17}$$

θ_{23} will be in the first (second) octant, i.e., the sign of ω will be positive (negative) if $\delta = 0$ (π). Recall, this corresponds to $x > 0$ ($x < 0$).

In Fig. 1 the global-fit 3σ range of $\sin\theta_{13}$ and $\tan 2\theta_{12}$ is shown as the blue dot-dashed box with the best-fit value indicated by

a black dot. Once the atmospheric and solar mass splittings are fixed, for any point within this region Eq. (15) determines a z, or equivalently an m_0, which leads to the correct solar splitting.

From the 3σ data [2] $\omega_{min} = 0$ for both octants and $\omega_{max} = 6.6°$ ($-8.3°$) for the first (second) octant. As $|\cos\delta| = 1$ for the real M_R case, in this model one has from Eq. (17) for both octants $|\omega| \geq 5.14°$ at 3σ. Thus the range of θ_{23} that can be obtained is rather limited.[4] The green solid (dashed) straight line is from Eq. (17) for ω_{max} for the first (second) octant. The region *below* this line is excluded in this model. Note that the best-fit point is permitted only for θ_{23} in the second octant.

Using the 3σ global-fit limits of θ_{13} and θ_{12}, from Eq. (15) one gets $z_{max} = 6.03 \times 10^{-2}$ implying that $(m_0)_{max} = 3.10$ meV. Also, consistency with both Eqs. (17) at ω_{max} and (15) sets $z_{min} = 4.01 \times 10^{-2}$ (3.88×10^{-2}) for the first (second) octant corresponding to $(m_0)_{min} = 2.13$ (2.06) meV. If, as a typical example, $m_0 = 2.5$ meV is taken and the best-fit values of the solar and atmospheric mass splittings are used then Eq. (13) gives the red dotted curve in Fig. 1.

In summary, for real M_R the free parameters are m_0, m_D^2/xm_R and y with which the solar mass splitting, θ_{12}, θ_{13}, θ_{23} are reproduced for normal mass ordering. Inverted ordering cannot be accommodated.

Reverting now to the complex M_R in Eq. (4) one has in the mass basis in place of Eq. (5):

$$M'^{mass} = \frac{m_D^2}{\sqrt{2}xym_R}\begin{pmatrix} 0 & ye^{i\phi_1} & ye^{i\phi_1} \\ ye^{i\phi_1} & \frac{xe^{i\phi_2}}{\sqrt{2}} & \frac{-xe^{i\phi_2}}{\sqrt{2}} \\ ye^{i\phi_1} & \frac{-xe^{i\phi_2}}{\sqrt{2}} & \frac{xe^{i\phi_2}}{\sqrt{2}} \end{pmatrix}. \tag{18}$$

x and y are now positive. M' is no longer hermitian. This is addressed, as usual, by defining the hermitian combination $(M^0 + M')^\dagger(M^0 + M')$ and treating $M^{0\dagger}M^0$ as the unperturbed term and $(M^{0\dagger}M' + M'^\dagger M^0)$ as the perturbation to lowest order. The zero order eigenvalues are now $(m_i^{(0)})^2$ and the complex yet hermitian perturbation matrix is

$$(M^{0\dagger}M' + M'^\dagger M^0)^{mass} = \frac{m_D^2}{\sqrt{2}xym_R}\begin{pmatrix} 0 & 2m_1^{(0)}y\cos\phi_1 & yf(\phi_1) \\ 2m_1^{(0)}y\cos\phi_1 & \frac{2}{\sqrt{2}}m_1^{(0)}x\cos\phi_2 & -\frac{1}{\sqrt{2}}xf(\phi_2) \\ yf^*(\phi_1) & -\frac{1}{\sqrt{2}}xf^*(\phi_2) & \frac{2}{\sqrt{2}}m_3^{(0)}x\cos\phi_2 \end{pmatrix}, \tag{19}$$

where

$$f(\xi) = m^+\cos\xi - im^-\sin\xi \ . \tag{20}$$

The subsequent analysis is similar to the one for real M_R.

The perturbation which splits the degenerate solar sector is the 2×2 block of Eq. (19). The solar mixing angle now is

$$\tan 2\theta_{12} = 2\sqrt{2}\,\frac{y}{x}\,\frac{\cos\phi_1}{\cos\phi_2}\,. \tag{21}$$

The limits of Eq. (8) apply on the ratio $(y\cos\phi_1/x\cos\phi_2)$. Also, $(\cos\phi_1/\cos\phi_2)$ must be positive.

Including first order corrections the wave function $|\psi_3\rangle$ is

$$|\psi_3\rangle = \begin{pmatrix} \kappa f(\phi_1)/m^+ \\ \frac{1}{\sqrt{2}}(1 - \frac{\kappa}{\sqrt{2}}\frac{x}{y}\,f(\phi_2)/m^+) \\ \frac{1}{\sqrt{2}}(1 + \frac{\kappa}{\sqrt{2}}\frac{x}{y}\,f(\phi_2)/m^+) \end{pmatrix}. \tag{22}$$

[4] This range is excluded at 1σ for the first octant.

Now κ is positive (negative) for NO (IO). One immediately has

$$\sin\theta_{13}\cos\delta = \kappa\cos\phi_1\ ,$$
$$\sin\theta_{13}\sin\delta = \kappa\,\frac{m^-}{m^+}\sin\phi_1\ . \tag{23}$$

The sign of $\cos\delta$ is the same as (opposite of) $\mathrm{sgn}(\cos\phi_1)$ for normal (inverted) mass ordering. Further, $\sin\phi_1$ determines the combination $\sin\theta_{13}\sin\delta$ that appears in the Jarlskog parameter, J, a measure of CP-violation. Note, ϕ_2 plays no role in fixing the CP-phase δ.

It is seen that for normal ordering ($\kappa > 0$) the quadrant of δ is the same as that of ϕ_1. For inverted ordering ($\kappa < 0$) δ is in the first (third) quadrant if ϕ_1 is in the second (fourth) quadrant and *vice-versa*.

θ_{23} obtained from Eq. (22) is

$$\tan\theta_{23} = \frac{1 - \frac{\kappa}{\sqrt{2}}\frac{x}{y}\cos\phi_2}{1 + \frac{\kappa}{\sqrt{2}}\frac{x}{y}\cos\phi_2}\ , \tag{24}$$

where, using Eqs. (21) and (23),

$$\tan\omega = \frac{2\sin\theta_{13}\cos\delta}{\tan 2\theta_{12}}\,. \tag{25}$$

Eq. (17) is recovered when $\cos\delta = \pm 1$. From Eq. (25), if δ lies in the first or the fourth quadrant – which yield opposite signs of J – θ_{23} is in the first octant while it is in the second octant otherwise.

A straight-forward calculation after expressing m_D and m_R in terms of $\sin\theta_{13}\cos\delta$, yields

$$\Delta m^2_{solar} = \mathrm{sgn}(\cos\phi_2)\, m^- m_1^{(0)}\,\frac{4\sin\theta_{13}\cos\delta}{\sin 2\theta_{12}}\,, \tag{26}$$

which bears a strong similarity with Eq. (13) for real M_R. Eqs. (14) and (15) continue to hold. To ensure the positivity of Δm^2_{solar}, noting the factors determining the sign of $\cos\delta$, one concludes that $\mathrm{sgn}(\cos\phi_1\cos\phi_2)$ must be positive for both mass orderings. Thus, satisfying the solar mass splitting leaves room for either octant of θ_{23} for both mass orderings. The allowed range of δ can be easily read off if we reexpress Eq. (15) as:

$$|\cos\delta| = \left(\frac{\Delta m^2_{solar}}{|\Delta m^2_{atm}|}\right)\left(\frac{\sin 2\theta_{12}}{4\sin\theta_{13}\,z}\right)\ . \tag{27}$$

In the following m_0, θ_{13}, and θ_{12} are taken as inputs and δ and θ_{23} are obtained using Eqs. (27) and (25). From these the CP-violation measure, J, and the combination $|m_{\nu_e\nu_e}|$ which determines the rate of neutrinoless double beta decay are calculated.

In the left panel of Fig. 2 is shown (thick curves) the dependence of θ_{23} on the lightest neutrino mass m_0 when the neutrino mass square splittings and the angles θ_{13} and θ_{12} are varied over their allowed ranges at 3σ. The thin curves correspond to taking the best-fit values. The green (pink) curves are for normal (inverted) mass ordering while solid (dashed) curves are for solutions in the first (second) octant. For inverted ordering the thick and thin curves are very close and cannot be distinguished in this figure. Notice that the 3σ predictions from this model are not consistent with $\theta_{23} = \pi/4$. As expected from Eq. (25), θ_{23} values are symmetrically distributed around $\pi/4$. Its range for inverted ordering falls outside the 1σ global fits but is consistent at 3σ. An improvement in the determination of θ_{23} will be the easiest way to exclude one of the orderings unless one is in the quasidegenerate regime. For normal ordering the smallest value of m_0 is determined by the 3σ limits of θ_{23} in the two octants. Eq. (26) permits arbitrarily small m_0 for inverted mass ordering (see below).

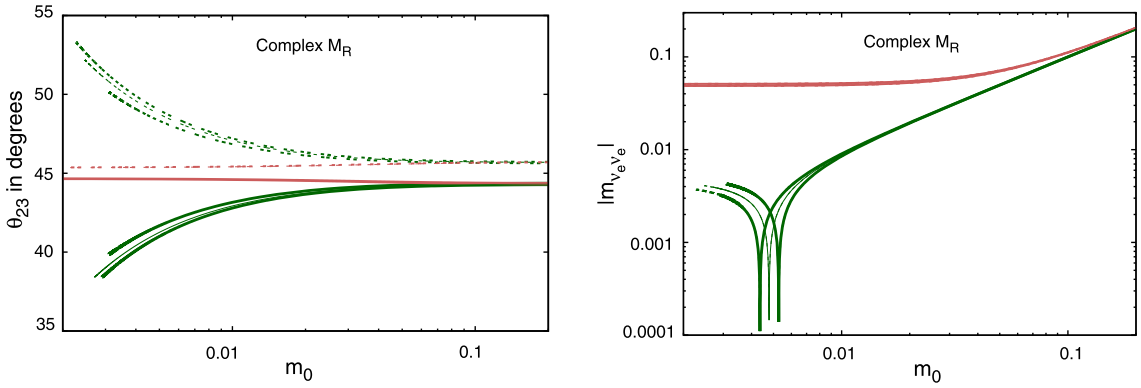

Fig. 2. θ_{23} ($|m_{\nu_e\nu_e}|$ in eV) as a function of the lightest neutrino mass m_0 (in eV) is shown in the left (right) panel. The green (pink) curves are for the normal (inverted) mass ordering. For every plot the region allowed at 3σ is between the thick curves while the thin curves are for the best-fit values of the inputs. The solid (dashed) curves correspond to the first (second) octant of θ_{23}. (For interpretation of the references to colour in this figure legend, the reader is referred to the web version of this article.)

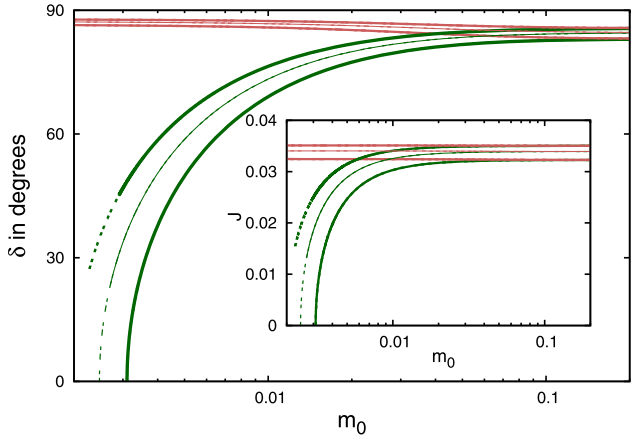

Fig. 3. The CP-phase δ is plotted as a function of m_0 (in eV). Inset: The leptonic CP-violation measure J is shown. The conventions are the same as that of Fig. 2.

In the right panel of Fig. 2 $|m_{\nu_e\nu_e}|$ has been plotted. The sensitivity of direct neutrino mass measurements is expected to reach around 200 meV [7] in the near future. Planned neutrinoless double beta decay experiments will also probe the quasidegenerate range of m_0 [8]. As can be seen from this figure, to distinguish the two mass orderings at least a further one order improvement in sensitivity will be needed. Long baseline experiments or large atmospheric neutrino detectors such as INO will settle the mass ordering more readily.

In Fig. 3 is displayed the variation of δ with m_0 for both mass orderings while J is shown in the inset. The conventions are the same as in Fig. 2. The sign of J is positive if δ is in the first or second quadrant and is negative for the other cases. As noted, the quadrant of δ (and the associated sign of J) can be altered by the choice of the quadrant of ϕ_1. However, from Eq. (27) for these alternatives, namely, $\pm\delta$ and $(\pi \pm \delta)$, the dependence of $|\cos\delta|$ on m_0 is the same for a particular mass ordering. With this proviso in mind, Fig. 3 has been plotted keeping δ in the first quadrant and J has been taken as positive.

J, which is proportional to $\sin 2\theta_{23}$, has no dependence on the octant of θ_{23} as the latter is symmetrical around $\pi/4$. In both Figs. 2 and 3, for normal ordering a slightly larger range of m_0 is allowed when θ_{23} is in the second octant. For the region where both octants are allowed the curves in Fig. 3 completely overlap. For inverted mass ordering both δ and J remain nearly independent of m_0.

For m_0 smaller than 10 meV, the CP-phase δ is significantly larger for inverted ordering.[5] This could provide a clear test of this model when the mass ordering is known and CP-violation in the neutrino sector is measured. The real limit ($\delta = 0$) is seen to be admissible, as expected from Fig. 1, only for normal ordering and that too not for the entire 3σ range, with the second octant allowing a larger region.

Since $0 \le z \le 1/2$ for NO and $1/2 \le z \le 1$ for IO, the allowed values of δ in the two orderings as seen from Eq. (27) are complementary tending towards a common value as $z \to 1/2$, the quasidegenerate limit, which begins to set in from around $m_0 = 100$ meV. The main novelty from the real M_R case is that in Eq. (15) by choosing $\cos\delta$ sufficiently small one can make $z \equiv m^- m_1^{(0)}/\Delta m^2_{atm} \sim 1$ so that solutions exist for m_0 for inverted mass ordering corresponding to even vanishing m_0 unlike the case of normal ordering where the lower limit of m_0 is set by $\cos\delta = 1$, i.e., real M_R.

We have checked that the size of the perturbation is at most around 20% of the unperturbed contribution for all cases.

In conclusion, a model for neutrino masses has been proposed in which the atmospheric mass splitting together with $\theta_{23} = \pi/4$ has an origin different from that of the solar mass splitting, θ_{12}, θ_{13}, and $\omega = \pi/4 - \theta_{23}$, all of which arise from a single perturbation resulting from a Type-I see-saw. The global fits to the mass splittings, θ_{12} and θ_{13} completely pin-down the model and the CP-phase δ and the octant of θ_{23} are predicted in terms of the lightest neutrino mass m_0. Both mass orderings are allowed, the inverted ordering being associated with near-maximal CP-violation. Both octants of θ_{23} can be accommodated. Further improvements in the determination of θ_{23}, a measurement of the CP-phase δ, along with a knowledge of the neutrino mass ordering will put this model to tests from several directions.

Acknowledgements

SP acknowledges a Senior Research Fellowship from CSIR, India. AR is partially funded by the Department of Science and Technology Grant No. SR/S2/JCB-14/2009.

References

[1] For the present status of θ_{13} see presentations from Double Chooz, RENO, Daya Bay, MINOS/MINOS+ and T2K at Neutrino 2014, https://indico.fnal.gov/conferenceOtherViews.py?view=standard&confId=8022.

[5] In fact for inverted ordering δ remains close to $\pi/2$ or $3\pi/2$ for all m_0.

[2] M.C. Gonzalez-Garcia, M. Maltoni, J. Salvado, T. Schwetz, J. High Energy Phys. 1212 (2012) 123, arXiv:1209.3023v3 [hep-ph], NuFIT 1.3 (2014).

[3] D.V. Forero, M. Tortola, J.W.F. Valle, Phys. Rev. D 86 (2012) 073012, arXiv:1205.4018 [hep-ph].

[4] P. Minkowski, Phys. Lett. B 67 (1977) 421;
M. Gell-Mann, P. Ramond, R. Slansky, in: F. van Nieuwenhuizen, D. Freedman (Eds.), Supergravity, North Holland, Amsterdam, 1979, p. 315;
T. Yanagida, in: Proc. of the Workshop on Unified Theory and the Baryon Number of the Universe, KEK, Japan, 1979;
S.L. Glashow, NATO Sci. Ser. B 59 (1980) 687;
R.N. Mohapatra, G. Senjanović, Phys. Rev. D 23 (1981) 165.

[5] Earlier work on neutrino mass models in which a few elements dominate over others can be traced to F. Vissani, J. High Energy Phys. 9811 (1998) 025, arXiv:hep-ph/9810435;
Models with somewhat similar points of view as those espoused here are E.K. Akhmedov, Phys. Lett. B 467 (1999) 95, arXiv:hep-ph/9909217;
M. Lindner, W. Rodejohann, J. High Energy Phys. 0705 (2007) 089, arXiv:hep-ph/0703171.

[6] For more recent work after the determination of θ_{13} see, for example, B. Brahmachari, A. Raychaudhuri, Phys. Rev. D 86 (2012) 051302, arXiv:1204.5619 [hep-ph];
B. Adhikary, A. Ghosal, P. Roy, Int. J. Mod. Phys. A 28 (2013) 1350118, arXiv:1210.5328 [hep-ph];
D. Aristizabal Sierra, I. de Medeiros Varzielas, E. Houet, Phys. Rev. D 87 (2013) 093009, arXiv:1302.6499 [hep-ph];
R. Dutta, U. Ch, A.K. Giri, N. Sahu, Int. J. Mod. Phys. A 29 (2014) 1450113, arXiv:1303.3357 [hep-ph];
L.J. Hall, G.G. Ross, J. High Energy Phys. 1311 (2013) 091, arXiv:1303.6962 [hep-ph];
T. Araki, Prog. Theor. Exp. Phys. 2013 (2013) 103B02, arXiv:1305.0248 [hep-ph];
M.-C. Chen, J. Huang, K.T. Mahanthappa, A.M. Wijangco, J. High Energy Phys. 1310 (2013) 112, arXiv:1307.7711 [hep-ph];
S. Pramanick, A. Raychaudhuri, Phys. Rev. D 88 (2013) 093009, arXiv:1308.1445 [hep-ph];
B. Brahmachari, P. Roy, J. High Energy Phys. 1502 (2015) 135, arXiv:1407.5293 [hep-ph].

[7] M. Haag, KATRIN Collaboration, PoS EPS-HEP2013 (2013) 518.

[8] W. Rodejohann, Int. J. Mod. Phys. E 20 (2011) 1833, arXiv:1106.1334 [hep-ph].